

Aircraft magnetic noise sources

J. Bradley Nelson, Defence Research & Development Canada - Atlantic, PO Box 1012, Dartmouth, Nova Scotia, Canada B2Y 3Z7

Copyright 2003, SBGf -Sociedade Brasileira de Geofisica

This paper was prepared for presentation at the 8th International Congress of The Brazilian Geophysical Society, held in Rio de Janeiro, Brazil, September 14-18, 2003.

Contents of this paper were reviewed by The Technical Committee of The 8th International Congress of The Brazilian Geophysical Society and do not necessarily represent any position of the SBGf, its officers or members. Electronic reproduction, or storage of any part of this paper for commercial purposes without the written consent of The Brazilian Geophysical Society is prohibited."

Abstract

Aeromagnetic aircraft and data acquisition systems generate magnetic interference which can effect the quality of the data collected. Many people believe that traditional aircraft compensation, which models the permanent, induced, and eddy-current sources, can remove all of this interference. However, survey aircraft are not perfectly rigid bodies, have moving ferrous parts, and have changing electrical configurations. In addition, as magnetometers become more sensitive, their non-linear behaviour may become important, and data acquisition systems can generate specific types of noise. This paper looks at a variety of aircraft noise sources that do not fit the traditional compensation models, and how they have been dealt with on the National Research Council Convair 580 aircraft.

1. Introduction

"Aircraft compensation" is the term usually applied to the modeling and removal of aircraft-generated magnetic noise due to permanent, induced, and eddy-current sources. These models assume that the airframe is rigid and that there is no hysteresis in the ferrous components of the aircraft (Leliak, 1961). The aircraft-noise model is usually built up from vector magnetometer signals which measure the components of the Earth's magnetic field in the aircraft axes, or from the pitch, roll, and yaw measurements. Traditional aircraft compensation is well understood and commercial products are available to perform this noise-removal in real time.

However, real aircraft are not perfectly rigid bodies and there a number of other sources for magnetic interference that are not accounted for by the standard model. The purpose of this paper is to describe a number of these non-traditional magnetic sources, and to show how they have been accounted for on the National Research Council Convair 580 aeromagnetic research aircraft.

2. Aircraft noise sources

2.1 Large interfering fields

The standard aircraft compensation models assume that the interfering field is much smaller than the Earth's field and can be approximated as

$$B_{\text{interference}} = | \mathbf{B}_{\text{Earth}} + \mathbf{B}_{\text{Aircraft}} | - | \mathbf{B}_{\text{Earth}} | \quad (1)$$

$$\sim [\mathbf{B}_{\text{Aircraft}} \cdot \mathbf{B}_{\text{Earth}}] / | \mathbf{B}_{\text{Earth}} | .$$

Figure 1 shows the accuracy of this approximation for the case when $\mathbf{B}_{\text{Aircraft}}$ and $\mathbf{B}_{\text{Earth}}$ are perpendicular to each other (i.e. where Equation (1) indicates that $B_{\text{interference}}$ is zero) and the Earth's field is 50000 nT.

Figure 1 indicates that in order to obtain aircraft compensation to the level of a few pT, it is necessary to either change the compensation model or to reduce the aircraft interference field to a few nT. The interference fields at the wingtip magnetometer locations on the Convair is ~ 5 nT so this is not a problem. However, the interference at the tail position is ~ 250 nT and thus limits the effectiveness of conventional compensation.

2.2 Propellers

The propellers on the Convair 580 are made of aluminum, and are therefore non-magnetic, but they will have eddy-currents flowing in them. In addition, there are steel components within the shaft and propeller assemblies that rotate at the same rate. Thus, one should expect magnetic signals at the wingtips (~13 m away) at the propeller rotation rate of 1020 RPM = 17 Hz . There may also be harmonics of 17 Hz detectable, in particular 68 Hz since the propellers have four blades.

2.3 Engines

The engines of the Convair run at a constant rate of 13,782 RPM and, because there are steel components within the engines which are rotating at this rate, one should expect magnetic noise at $(13782/60) = 229.7 \text{ Hz}$ + harmonics. The sampling rate of the Convair was chosen to be 160 Hz in order to ensure that neither the propeller or engines frequencies aliased back near DC.

2.4 Aircraft power

Aircraft power in the Convair 580 is available at 28 Volts DC, 115 Volts at 60 Hz, and 115 Volts at 400 Hz. Generators on each engine produce the 28 Volts DC, but because the brushes can make intermittent contact, there are many small spikes in the output. For this reason, all project equipment is operated from 60 Hz regulated power supplies.

Neither the 400 Hz, which comes directly from the alternators on each engine, nor the 60 Hz, which comes from the 400-60 Hz inverters, are pure waveforms. Although there does not appear to be much amplitude or phase variation, there are many harmonics present in both the 60 and 400 Hz supplies. In addition, the actual frequency of the 400 Hz power in the Convair 580 is 393.5 Hz because frequency is derived from the engine RPM. Thus, one should expect there to be measurable magnetic fields at 60, 120, 180, 240,Hz and ~400, ~800, ~1200, ... Hz at the magnetometers. These fields will create discrete lines in the PSD but the actual frequency of these lines will depend on the sampling rate.

Even though higher frequencies will alias back, the amplitude of those aliased lines (A_{aliased}) will be diminished by a factor of:

$$A_{\text{aliased}} = A_{\text{actual}} \times \sin(\pi FT) / [FT] \quad (2)$$

where F = the actual frequency in Hz,
 $T = 1/(\text{Sampling Rate})$, and
 A_{actual} = the amplitude of the actual signal.

Thus the amplitude of the magnetic fields measured at the higher harmonics will be significantly reduced from that of the fundamental.

Table 1 gives the aliased frequencies for the harmonics of the power lines for a sampling rate of 160 Hz. Only the 8th harmonic of 60 Hz will alias back into the band 0-1 Hz and the 2nd harmonic of 393.6 Hz will alias back into the band 1-20 Hz. Airborne measurements have shown that only the 12.8 Hz line is barely detectable.

Table 1. Aliased power frequencies in the Convair 580 at a sampling rate of 160 Hz.

Actual Frequency (Hz)	Aliased Frequency (Hz)
60 x 1 = 60	60
60 x 2 = 120	40
60 x 3 = 180	20
60 x 4 = 240	80
60 x 5 = 300	20
60 x 6 = 360	40
60 x 7 = 420	60
60 x 8 = 480	DC
60 x 9 = 540	60
393.6 x 1 = 393.6	73.6
393.6 x 2 = 787.2	12.8
393.6 x 3 = 1180.8	60.8
393.6 x 4 = 1574.4	25.6
393.6 x 5 = 1968.0	48.0
393.6 x 6 = 2361.6	38.4
393.6 x 7 = 2755.2	35.2

2.5 Vibration

Vibration can cause noise in three different ways:

- 1) by direct modulation of the Larmor signal if the optical alignment inside the magnetometer is poor or optical components are slightly loose,
- 2) by motion of the sensor through gradients in the ambient magnetic field. These gradients could be due to the Earth's field or the aircraft,
- 3) if the sources move relative to the magnetometer.

Whatever the source, one may expect magnetic noise at frequencies corresponding to motion of the magnetometers and vibration modes of the aircraft itself. In the case of the wingtip magnetometers on the Convair, both the wing flex and the aircraft phugoid motion will produce predominantly vertical motion. There may also be a small horizontal component as the prop-synching causes the aircraft to oscillate slightly about the yaw axis. In the case of the tail magnetometer, the motion will be vertical (phugoid), horizontal transverse (fuselage and tail bending), and horizontal longitudinal (the pitch motion associated with phugoid motion). Table 2, taken from MacLellan, 1952 gives the vibration frequencies of the wings, tail, and fuselage as measured on a Convair 340. Vibration frequencies in the Convair 580 are expected to be similar.

It should be noted that none of the expected resonance frequencies given in Table 2 are near the propeller frequency (17 Hz) or the blade frequency (4x17 Hz=68 Hz).

Figure 2 shows the typical power spectral densities from all four Convair magnetometers in turbulent flight. Three of the Convair's magnetometers are mounted in wingpods which have natural resonances near 17 Hz and are driven by the propeller vibration. The sources for the other discrete and broad-band noise can be found in Tables 1 and 2.

Table 2. Vibration frequencies measured in a Convair 340 (from MacLellan, 1952).

Frequency (Hz)	Type of Excitation	Characteristics of Mode
2.88	Symmetric Wing	Symmetric Wing Bending
4.28	Anti-symmetric Wing	Wing Anti-symmetric Bending
4.83	Symmetric Wing	Wing Symmetric Torsion
5.05	Anti-symmetric Wing	Fuselage Side Bending
7.03	Anti-symmetric Wing	Wing Anti-symmetric Torsion
7.53	Symmetric Wing	Stabilizer Symmetric Bending
7.87	Anti-symmetric Wing	Stabilizer Anti-symmetric Bending
9.10	Anti-symmetric Wing	Fuselage Torsion
10.30	Symmetric Wing	Fuselage Vertical Bending
11.67	Anti-symmetric Wing	Fin Bending
28.33	Symmetric Wing	Stabilizer Symmetric Torsion
29.50	Anti-symmetric Wing	Stabilizer Anti-symmetric Torsion
38.50	Anti-symmetric Wing	Fin Torsion
3.72	Symmetric Elevator	Elevator Symmetric Rotation
4.67	Rudder	Rudder Rotation
5.72	Symmetric Wing	Aileron Symmetric Rotation
5.90	Symmetric Wing	Powerplant
10.00	Rudder	Rudder Flight Tab Rotation
12.33	Anti-symmetric Elevator	Elevator Anti-symmetric Rotation
13.83	Anti-symmetric Wing	Rudder Torsion
33.33	Symmetric Elevator	Elevator Servo Tab Rotation
40.83	Rudder	Rudder Trim Tab Rotation
42.83	Symmetric Elevator	Elevator Servo Trim Tab Rotation
47.00	Symmetric Wing	Aileron Tab Rotation
51.33	Anti-symmetric Elevator	Elevator Anti-symmetric Torsion
59.00	Symmetric Elevator	Elevator Symmetric Torsion

Vertical accelerometers have been mounted in the wingpods of the Convair and post-processing algorithms have been developed to remove the magnetic noise that correlates with the accelerometer data.

2.6 Electrical pick-up on wiring

The wingtip magnetometers in the Convair are connected to the data acquisition system by approximately 20 m of cable. Electrical pick-up may be expected, even with proper grounding. This can effect the threshold crossings, and thus the time-tags, and magnetic field measurements. The sources of the electrical pick-up include:

- 1) electronics aboard the aircraft,
- 2) external radio, VHF, and radar signals,
- 3) the engines, and
- 4) the generators.

Experiments showed that significant electrical pickup does exist on the Convair's wing wiring. To reduce this effect, the Larmor signal is taken from the TTL output of the CS-2 magnetometers. In addition, tri-axial cables are used wherever possible to provide extra shielding.

2.7 Control surface motion

The cesium magnetometers in the Convair 580 are located quite close to the control surfaces - the wingtip magnetometers are located 1-2 m from the ailerons and the tail magnetometer is approximately 50 cm from the rudder. If these control surfaces, or the hinges on which they pivot, contain ferromagnetic or conductive components, then they will generate magnetic fields when they move. These signals will not be compensable with the rigid-airframe compensation models described previously.

A series of measurements were taken on the ground (with both the engines and auxiliary power unit turned off) to determine the size of the signals due to control surface movements. The surfaces were moved from full positive to full negative setting every 5 seconds and the outputs of the various magnetometers were monitored. The signals observed were "square-waves", indicating that the sources were ferromagnetic, not eddy currents. The aircraft was on a roughly magnetic south heading. Because of extraneous magnetic noise in the hangar, it was not possible to measure signals smaller than 0.05 nT. Table 3 summarizes those measurements. Clearly there are significant magnetic signals caused by moving ferromagnetic components within the control surfaces.

Table 3. Noise produced by control surface movements, as measured on the ground.

Magnetometer	Aileron	Rudder	Elevator
Port Forward	0.3 nT	not detected	not detected
Port Aft	0.5 nT	not detected	not detected
Starboard	0.2 nT	not detected	not detected
Tail	not detected	0.5 nT	0.1 nT

The Convair control surfaces have been instrumented. An adaptive algorithm, which removes the magnetic noise that correlates with the control surface movements, has been developed and is used in post-processing.

2.8 Electrostatic buildup/discharge

There are two major sources of electrostatic buildup on aircraft - precipitation (Jay 1988) and fuel combustion in the engines (Nanevicz 1975). It has been shown that potentials of 25-60 kV are quite common on a variety of aircraft and these potentials often lead to noise in navigation or communication systems. Static dischargers (or "wicks") are usually mounted along the control surfaces to dissipate this static buildup. Quasi-continuous discharge currents of a few micro-Amperes are typical, but much larger currents (milli-Amperes) have been reported (Nanevicz 1975). The discharge currents are a series of miniature sparks that last a very short time but occur almost continuously.

In order to reduce the noise from electrostatic buildup/discharge, it is very important to provide a conductive path to the discharge wicks. In the Convair, conductive tape is placed along the inside of the fiberglass wingpods from the leading endcap all the way to the discharge wick at the end of the pod. Figure 3 shows the electrostatic discharge spikes produced when

the Convair was flown through high stratus clouds, and the conductive tape had been torn.

2.9 Generator brushes

In-flight measurements showed that the magnetic field measured by the Convair's port magnetometers (especially the port rear) had many small amplitude, short-duration, spikes. This led to the generally higher white noise floor for the port magnetometers vs the starboard magnetometer seen in Figure 2. One possible mechanism for creating these short duration spikes is worn brushes within the generators making intermittent contact. The port generator bushes were replaced and Figure 4 compares the port aft magnetometer signal before and after the brush replacement. The "thick" bands in Figure 4 are just the envelopes of the 17, 60, and 67-74 Hz signals described in the previous section. Looking only at the transients that stick out above and below these bands, there appears to be a reduction in the amplitude of the spikes when generator brushes were replaced. Figure 4. Total-field measured by the port aft magnetometer with the old generator brushes (black) vs new generator brushes (red).

2.10 Avionics

The UHF and VHF radios generate small steps in the total-field signals measured by the wingtip magnetometers on the Convair. A post-processing algorithm has been developed and tested for removing these steps, based on a simple ON/OFF flag. This algorithm will be coded and implemented as part of the real-time compensation.

2.11 Hysteresis

A compensation model to account for hysteresis in the ferromagnetic components of the Convair was developed in the mid 1990's (Nelson and Hardwick, 1996). However, it was found to be difficult to implement and the improvement was not substantial. We have not chosen to use this model as adaptive compensation models appear to work just as well and are simpler to implement.

3. Conclusions

A number of aircraft noise sources that cannot be removed by standard aircraft compensation have been identified on the NRC Convair 580 aircraft. In some cases, such as the electrostatic buildup, generator brushes, and electrical pickup, modifications were made to the aircraft. In other cases, such as vibration and control surface motion, auxiliary sensors were installed and used to remove correlated noise. Finally, the spectral characteristics of the in-flight magnetic noise were used to identify the optimum sample rate such that high-frequency noise did not alias back into the bandwidth of interest.

4. References

Cline, Jay, D., Electrostatic Charging in Flight, Avionics, August 1988.

Aircraft magnetic noise sources

Leliak, P., Identification and Evaluation of Magnetic Field Sources of Magnetic Airborne Detector Equipped Aircraft, Inst. Radio Eng. Trans, Aerospace and Navigational Elect. **8**, 95-105, 1961.

MacLellan, A.D., Results of Model 340 Ground Vibration Test, Consolidated Vultee Aircraft Corporation, San Diego Division, Report ZU-340-006, February 1952.

Nanevicz, J.E., Flight-Test Studies of Static Electrification on a Supersonic Aircraft, in: Conference on Lightning and Static Electricity, Abingdon, Oxon, England, April 14-17, 1975, Proceedings. (A76-14402 03-01) London, Royal Aeronautical Society, 1975.

Nelson, J. Bradley and Hardwick, C.D., Modelling Hysteresis for Aeromagnetic Compensation, DREA Technical Memorandum 96/221, March 1996.

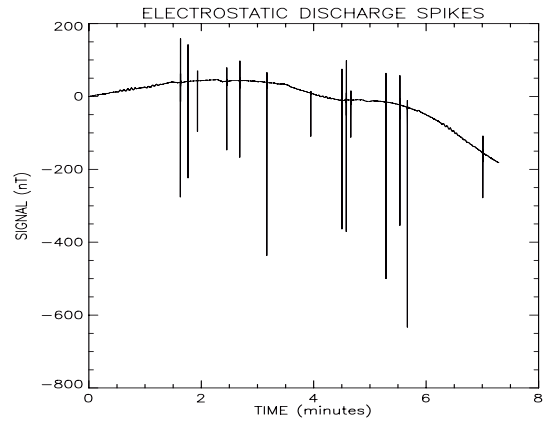


Figure 3. Spikes caused by electrostatic buildup/discharge when the conductive path was interrupted.

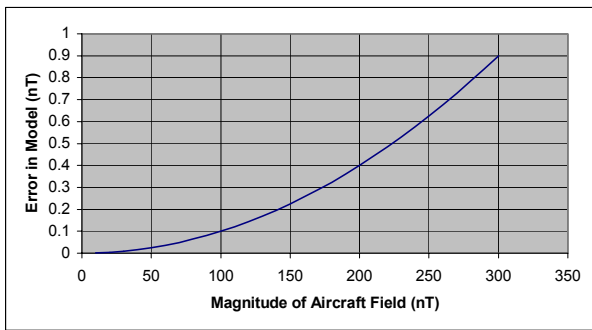


Figure 1. Accuracy of standard aircraft compensation model as a function of size of the aircraft's interfering field ($|\mathbf{B}_{\text{Earth}}| = 50000 \text{ nT}$).

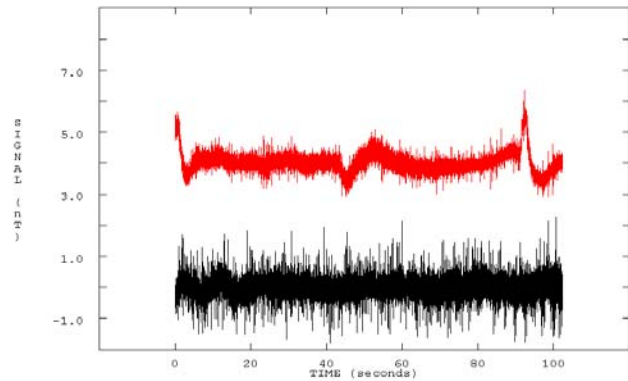


Figure 4. Total-field measured by the port aft magnetometer with the old generator brushes (black) vs new generator brushes (red).

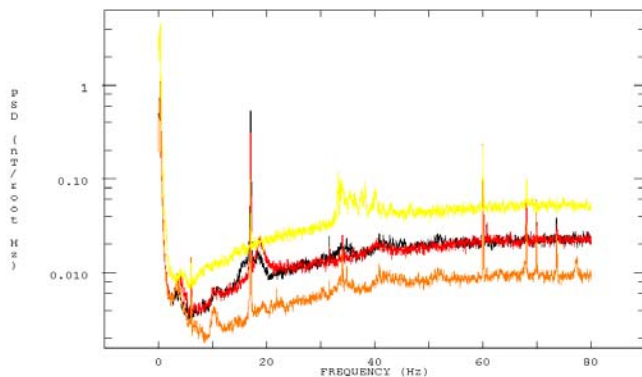


Figure 2. PSD's of the four cesium magnetometers on the Convair 580 measured in flight. Black=Port Fwd; Red=Port Aft; Orange=Stbd; Yellow=Tail.